

Figure 1: Compressed plot of ATMOs/Spacelab 3 spectra in the “atmospheric window” near $11 \mu\text{m}$ for three tangent heights. The absorption features of carbon dioxide, ozone, nitric acid, and two chlorofluorocarbons can be easily detected. The absorption due to sulfur hexafluoride at 947.9 cm^{-1} is not so easily discerned.

“Spectroscopy of the Earth’s Atmosphere and Interstellar Medium,” Edited by K. Narahari Rao and Alfons Weber, Academic Press, 1992.

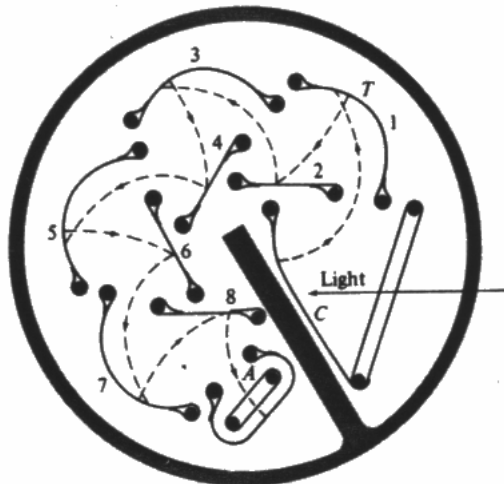


Figure 2: Photocathode and focusing dynode configuration of a typical commercial photomultiplier. C = cathode; 1-8 secondary-emission dynodes; A = collecting anode.

“Optical Electronics,” Fourth Edition, Amnon Yariv, Saunders College Publishing, 1991.

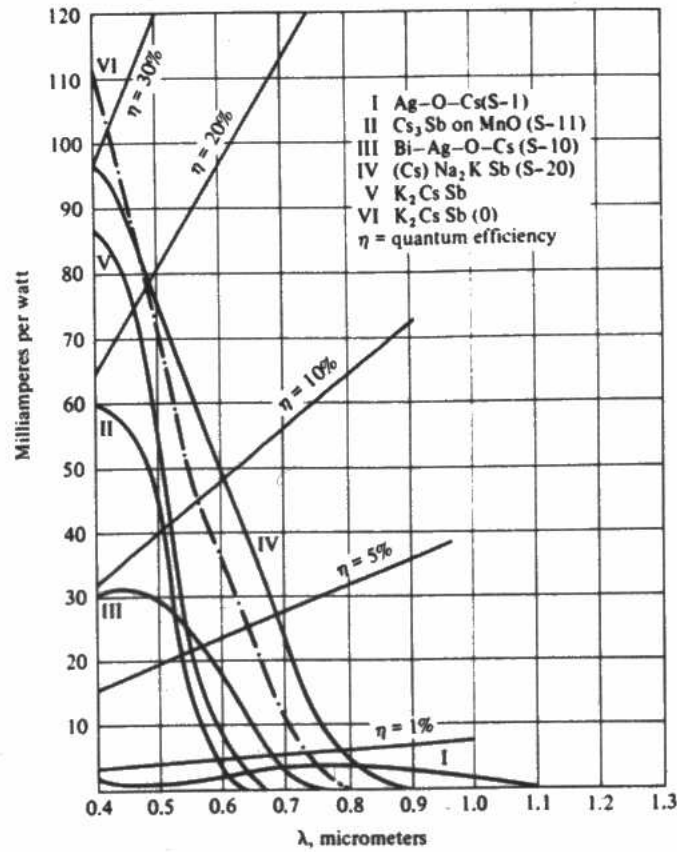


Figure 3: Photoresponse versus wavelength characteristics and quantum efficiency of a number of commercial photocathodes.

“Optical Electronics,” Fourth Edition, Amnon Yariv, Saunders College Publishing, 1991.

Band gap and longest detectable wavelength for selected semiconductors.		
Material	Band Gap (eV)	Longest wavelength (μm)
ZnS	3.6	0.345
CdS	2.41	0.52
CdSe	1.8	0.69
CdTe	1.5	0.83
Si	1.12	1.10
Ge	0.67	1.85
PbS	0.37	3.35
InAs	0.35	3.54
Te	0.33	3.75
PbTe	0.3	4.13
PbSe	0.27	4.58
InSb	0.18	6.90

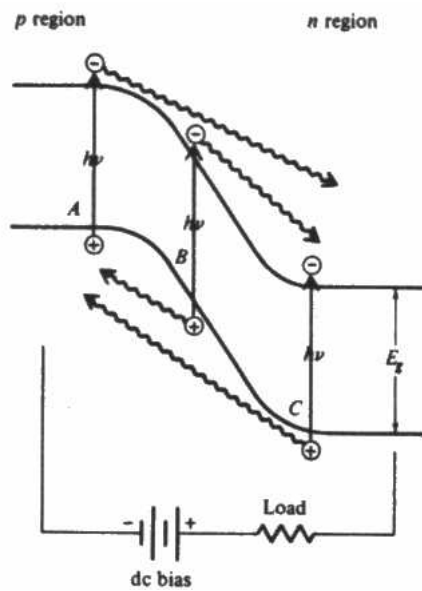


Figure 4: The three types of electron-hole pair creation by adsorbed photons that contribute to current flow in a $p - n$ photodiode.

“Optical Electronics,” Fourth Edition, Amnon Yariv, Saunders College Publishing, 1991.

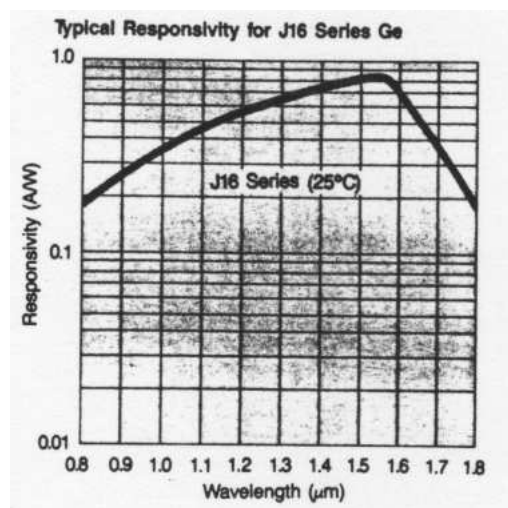


Figure 5: Typical germanium photodiode response curve.

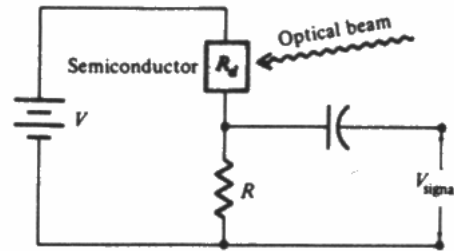


Figure 6: Typical biasing circuit of a photoconductive detector.

“Optical Electronics,” Fourth Edition, Amnon Yariv, Saunders College Publishing, 1991.

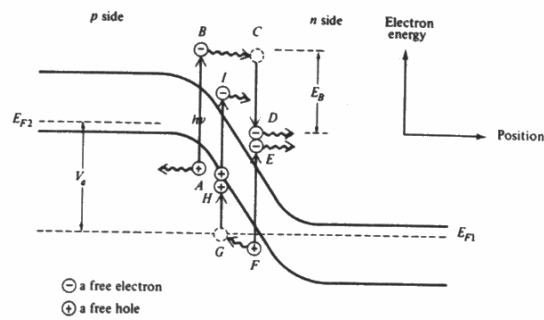


Figure 7: Energy-position diagram showing the carrier multiplication following a photon adsorption in a reverse-biased avalanche photodiode.

“Optical Electronics,” Fourth Edition, Amnon Yariv, Saunders College Publishing, 1991.

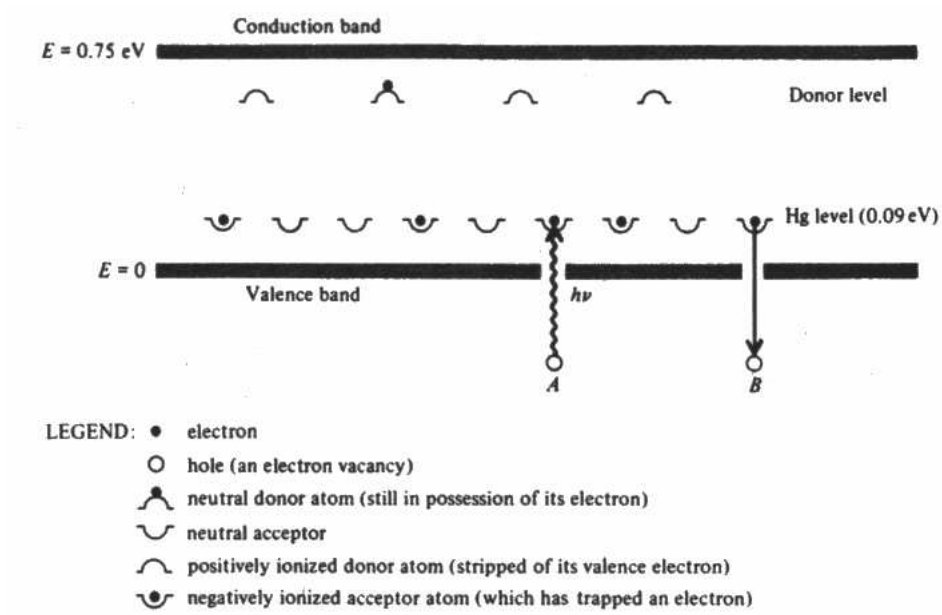


Figure 8: Donor and acceptor impurity levels involved in photoconductive semi-conductors.

“Optical Electronics,” Fourth Edition, Amnon Yariv, Saunders College Publishing, 1991.

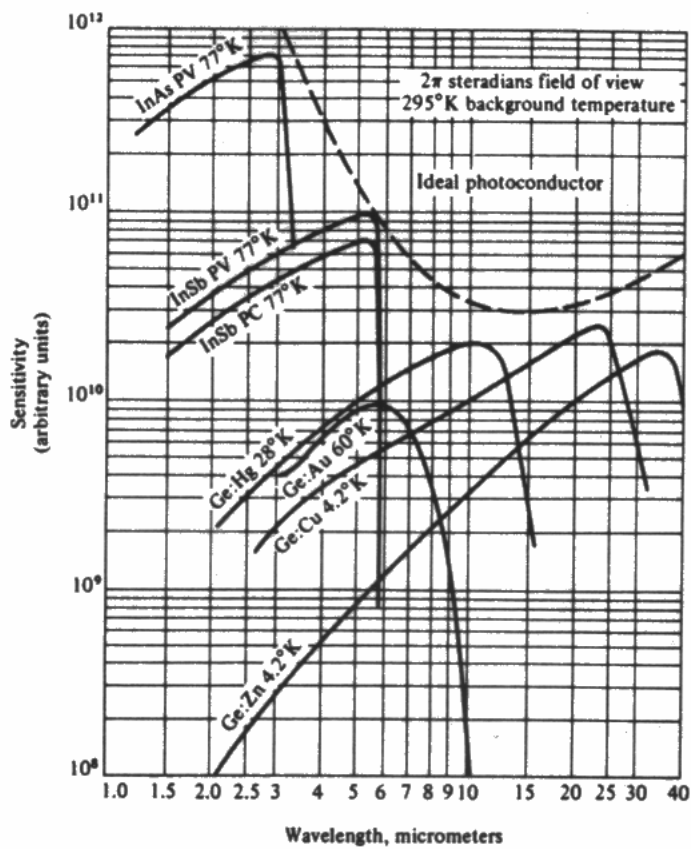


Figure 9: Relative sensitivity of a number of commercial photoconductors. "Optical Electronics," Fourth Edition, Amnon Yariv, Saunders College Publishing, 1991.

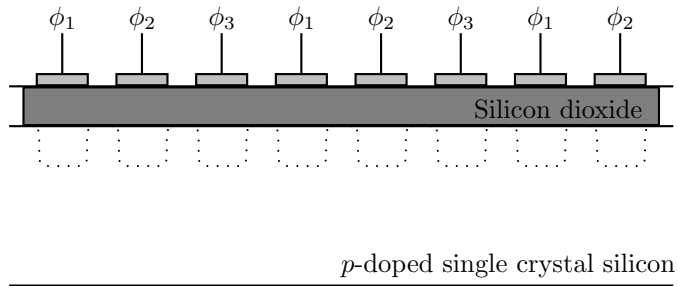


Figure 10: Schematic of a CCD image sensor and gating electrodes. Voltages applied on the electrodes serve to confine photogenerated minority charge carriers in the region near each electrode.

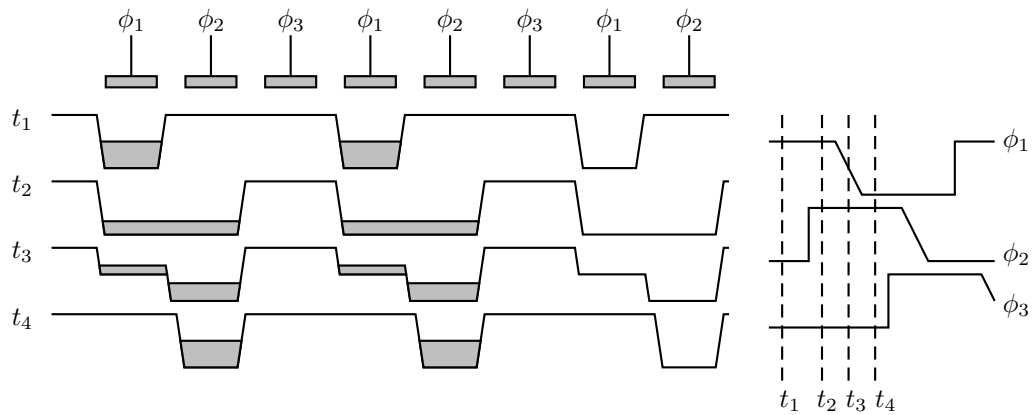


Figure 11: Charge flow in a 3 phase CCD shift register readout.